

## Evolution from a Fraunhofer to a Pearcey diffraction pattern

To cite this article: J F Nye 2003 *J. Opt. A: Pure Appl. Opt.* **5** 495

View the [article online](#) for updates and enhancements.

### You may also like

- [Propagation of a Pearcey beam in uniaxial crystals](#)  
Chuangjie Xu, , Ludong Lin et al.
- [Aberration-like cusped focusing in the post-paraxial Talbot effect](#)  
James D Ring, Jari Lindberg, Christopher J Howls et al.
- [Boundary asymptotics of non-intersecting Brownian motions: Pearcey, Airy and a transition](#)  
Thorsten Neuschel and Martin Venker

# Evolution from a Fraunhofer to a Pearcey diffraction pattern

J F Nye

H H Wills Physics Laboratory, University of Bristol, Tyndall Avenue, Bristol BS8 1TL, UK

Received 5 March 2003, accepted for publication 2 July 2003

Published 28 July 2003

Online at [stacks.iop.org/JOptA/5/495](http://stacks.iop.org/JOptA/5/495)

## Abstract

A cylindrical lens of small aperture produces in its focal plane a row of wave dislocations (phase singularities or optical vortices) as part of the Fraunhofer diffraction pattern for a slit. On the other hand, when the aperture is large, aberration produces a cusp caustic at the focus and its associated diffraction, namely, the Pearcey pattern. Passing smoothly from one extreme to the other shows that the Fraunhofer dislocations move to become the dislocations outside the caustic while the dislocations inside the caustic are created successively in pairs. The pairs are accompanied by phase saddles, as expected from previous work. Similar sequences would be expected for all the higher diffraction catastrophes. In this way the movement of the structurally stable dislocations forms a link between the structurally unstable line or point focus of engineering optics and the stable caustics of catastrophe optics.

**Keywords:** Diffraction, cusp, caustic, Fraunhofer, Pearcey, wave dislocations, singularity optics, optical vortices

## 1. Outline of the problem

The monochromatic diffraction pattern near the line focus of a cylindrical lens of small aperture is the well-known Fraunhofer pattern. On the other hand, if the aperture is large enough, cylindrical aberration becomes apparent; in geometrical optics this manifests itself as a cusp caustic, but on a finer scale as a diffraction pattern. The diffraction pattern associated with a cusp is described by the Pearcey integral of catastrophe optics (figure 1) (Pearcey 1946, Berry *et al* 1979, Connor and Farrelly 1981, Berry 1992, Nye 1999, NIST 2004). Thus, as the aperture is increased one passes continuously from the Fraunhofer to the Pearcey pattern. Singularity optics regards such patterns as largely characterized by their arrangements of phase singularities, or wave dislocations. Their topological nature ensures that wave dislocations cannot be created or destroyed, except in pairs. The purpose here is to trace how the single row of wave dislocations in the Fraunhofer pattern smoothly transforms itself into the rather more complicated two-dimensional arrangement of the Pearcey pattern.

## 2. The model

Rather than examine all possible combinations of focal length, aperture, aberration, and wavelength  $\lambda$ , we aim for a universal

sequence of diffraction patterns in terms of dimensionless variables, evolving under the control of a single dimensionless parameter. This is achieved by examining the limit  $\lambda \rightarrow 0$ . In this limit all the diffraction detail flows anisotropically towards the focus, the point of the cusp. Therefore it is sufficient to concentrate solely on the neighbourhood of the cusp point.

A model that contains the essence of the required evolution is as follows. In figure 2, a monochromatic scalar wave emerges from the aperture of a cylindrical lens system to produce an approximation to a point focus (in two dimensions) at the point  $F_0$ . The focal length is  $F$ . We use coordinates  $\xi'$ ,  $\zeta'$  with origin at the centre of the aperture, and coordinates  $x'$ ,  $z'$  with origin at  $F_0$  for an observation point P; thus  $\xi' = x'$ ,  $\zeta' = F + z'$ . The emerging wave has uniform amplitude (unity) across the aperture and its distribution of phase is specified as  $-kf(\xi')$ , where  $k = 2\pi/\lambda$ . The function  $f(\xi')$  is the height of the initial wavefront at  $Q = (\xi', 0)$  measured parallel to QP, whose direction is essentially that of  $QF_0$ . The disturbance at the point P is an integral of contributions (secondary cylindrical wavelets) from elements  $d\xi'$  of the aperture. Thus the complex amplitude at P is

$$\psi(P) = C \int_{-a'}^{a'} \rho^{-1/2} \exp[ik(\rho - f)] d\xi' \quad (1)$$

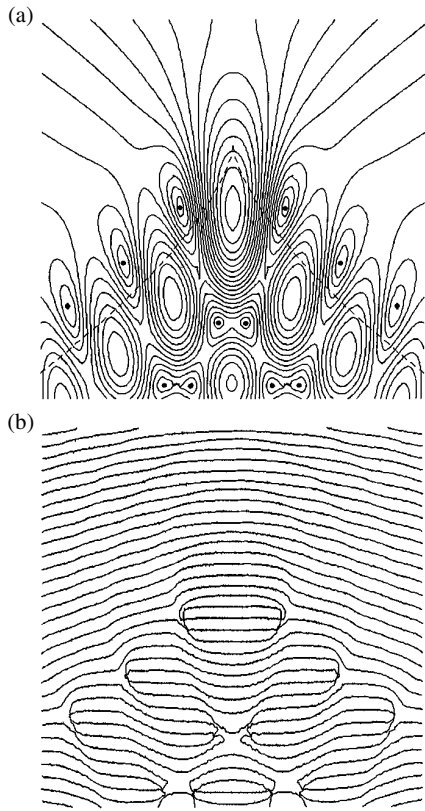


**Figure 1.** The cusp diffraction pattern: (a) amplitude (black dots mark the zeros), (b) phase. (Reproduced by permission from Berry (1992).)

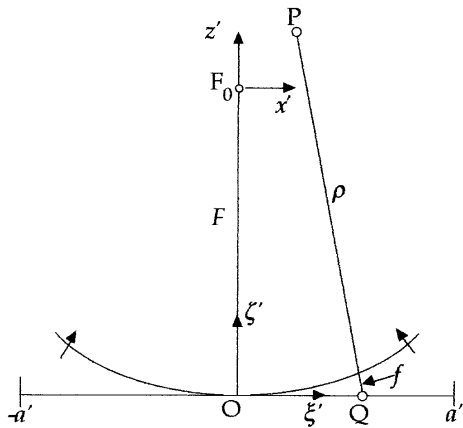


**Figure 2.** The observation point P receives contributions from elements  $d\xi'$  in the aperture, such as that at Q; the aperture extends from  $\xi' = -a'$  to  $a'$ .

where  $k\rho \gg 1$ ,  $C = (k/2\pi i)^{1/2}$ ,  $\rho$  is the distance PQ, and the aperture extends from  $\xi' = -a'$  to  $a'$ . The value of  $C$  is derived, for example, in Nye (1999, p 125).

We write the expression for  $\rho$  as  $\rho = \{(\zeta'^2 + (x' - \xi')^2)\}^{1/2}$  and, because we are interested in the cusp, expand the square root up to fourth powers, using the paraxial approximation,  $x' - \xi' \ll \zeta'$ , to give

$$\rho = \zeta' + \frac{(x' - \xi')^2}{2\zeta'} - \frac{(x' - \xi')^4}{8\zeta'^3}.$$

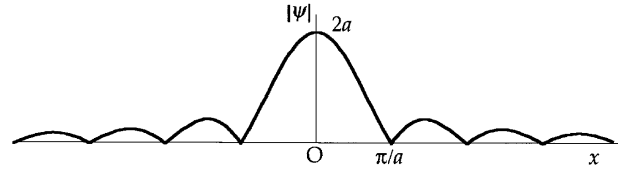


**Figure 3.** The Fraunhofer distribution of the amplitude in the focal plane.

The exponent in the integral is now  $ik\{-f(\xi') + \zeta' + \frac{(x' - \xi')^2}{2\zeta'} - \frac{(x' - \xi')^4}{8\zeta'^3}\}$ . Whereas  $f(\xi')$  is the height of the emerging wavefront relative to a straight line ( $\zeta' = 0$ ), we now define  $g(\xi')$  as the height relative to a circle centred on  $F_0$ , again measured parallel to QP. Thus  $g(\xi')$  is a measure of the aberration. Specifically, to fourth order,  $g(\xi') = f(\xi') - \frac{\xi'^2}{2F} + \frac{\xi'^4}{8F^3}$ . If we write  $X = \frac{x'}{\zeta'}$ ,  $Z = \frac{1}{2}(\frac{1}{F} - \frac{1}{\zeta'})$ ,  $\gamma = -\frac{1}{8}(\frac{1}{F^3} - \frac{1}{\zeta'^3})$ , and the distance OP as  $R = (\zeta'^2 + x'^2)^{1/2} \approx \zeta' + \frac{x'^2}{2\zeta'} - \frac{x'^4}{8\zeta'^3}$ , the exponent now takes the form

$$ikR - ik[g(\xi') + \gamma\xi'^4 + \dots + Z\xi'^2 + X\xi'].$$

The dots indicate higher-order terms that may be dropped because  $\xi' \ll \zeta'$  and  $x' \ll \zeta'$ ; specifically,  $\xi'(x'/\zeta')^3 \ll \xi'(x'/\zeta')$ ,  $(\xi'^2/\zeta')(x'/\zeta')^2 \ll \xi'^2/\zeta'$ , and  $(\xi'x'/\zeta')(\xi'/\zeta')^2 \ll (\xi'x'/\zeta')$ . The initial wave, which is determined by  $g(\xi')$ , is fixed and we will later take  $g(\xi') = \beta\xi'^4 + \text{higher terms in } \xi'$ . Thus, while  $\gamma$  depends on the position of the observation point P,  $g(\xi')$  does not. We have already noted that, as  $k \rightarrow \infty$ , the diffraction detail we are interested in becomes increasingly concentrated near the focus,  $\zeta' = F$ , where  $\gamma = 0$ . Thus the term  $\gamma\xi'^4$  becomes small compared with  $\beta\xi'^4$  and may be dropped. Again, because we are concerned only with the immediate neighbourhood of the focus, the factor  $\rho^{-1/2}$  in equation (1) may be taken outside the integral as a constant  $F^{-1/2}$  and the equation becomes

$$\psi(P) = CF^{-1/2}e^{ikR} \int_{-a'}^{a'} e^{-ik\phi} d\xi',$$

with

$$\phi = g(\xi') + Z\xi'^2 + X\xi'. \tag{2}$$

In terms of the coordinate  $z'$  measured from the focus,  $\zeta' = F + z'$  and  $z'$  is small. Expanding the expression for  $Z$  for small  $z'$ , we find  $Z = z'/2F^2$ . Thus  $X$  and  $Z$  are proportional to  $x'$  and  $z'$  respectively, that is, Cartesian coordinates for P with origin at  $F_0$ . Notice, however, that  $X$  and  $Z$  have different physical dimensions. Near enough to the focus the phase factor  $e^{ikR}$  is simply the plane wave  $e^{ik\zeta'} = e^{ik(F+z')} \approx e^{ik(F+2F^2Z)} = e^{ikF} e^{i\kappa Z}$ , where  $\kappa = 2F^2k$ .  $\kappa$  is a constant with dimensions of length. Equation (2) may now be written for the neighbourhood of the focus as

$$\psi(X, Z) \propto e^{i\kappa Z} \int_{-a'}^{a'} e^{-ik\phi} d\xi'. \tag{3}$$

Essentially we have moved from coordinates  $x', z'$  to  $X, Z$  and replaced the circular wave  $e^{ikR}$  in the prefactor by the plane wave  $e^{i\kappa Z}$ .

We now choose the function  $g(\xi')$ , which specifies the deviation of the emerging wavefront from the circular one that

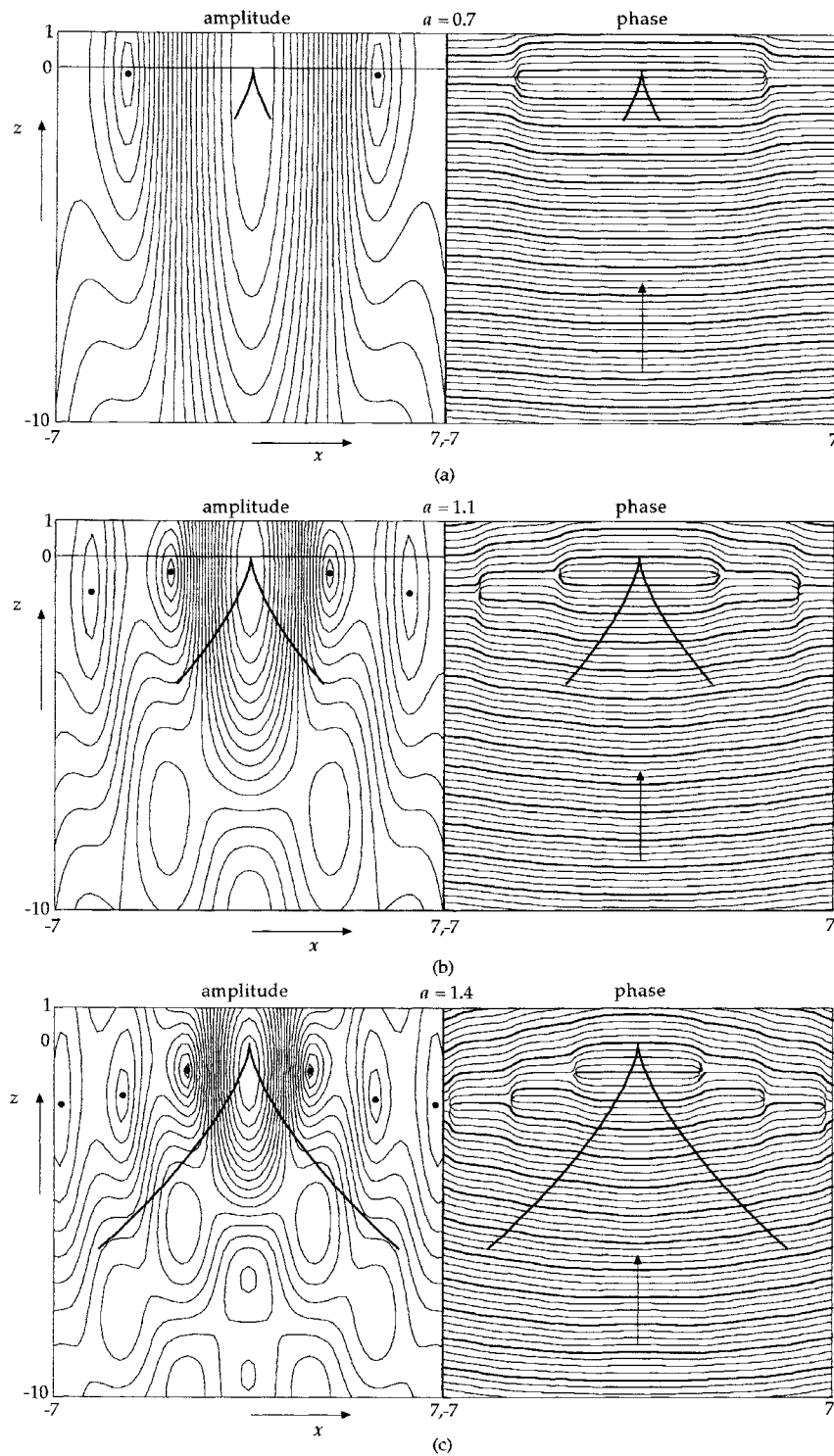


**Figure 4.** ((a)–(e)) Evolution of the pattern for the indicated values of  $a$  and  $K = 8$ . The left-hand half of each figure shows contours of amplitude and the right-hand half shows contours of phase (phase = 0 is bold). The arrows show the direction of increasing phase; the black dots mark zeros of the amplitude. The dislocations to the right of the caustic all have clockwise circulation; those to the left are anticlockwise.

would focus at  $F_0$ . Since we want to have a symmetrical cusp we omit a cubic term and write  $g(\xi') = \beta\xi'^4 + \dots$ , where the dots denote higher even-order terms in  $\xi'$ . Thus, from equation (2)  $\phi = (\beta\xi'^4 + \dots) + Z\xi'^2 + X\xi'$ . The principle of stationary phase tells us that, as we approach the limit  $k \rightarrow \infty$ ,

the range of  $\xi'$  contributing to the integral becomes more and more concentrated around  $\xi' = 0$ . Thus the higher terms represented by the dots can be ignored, but the term in  $\xi'^4$  must be retained to obtain a cusp. The remaining terms are recognized as the potential for a cusp in catastrophe theory.

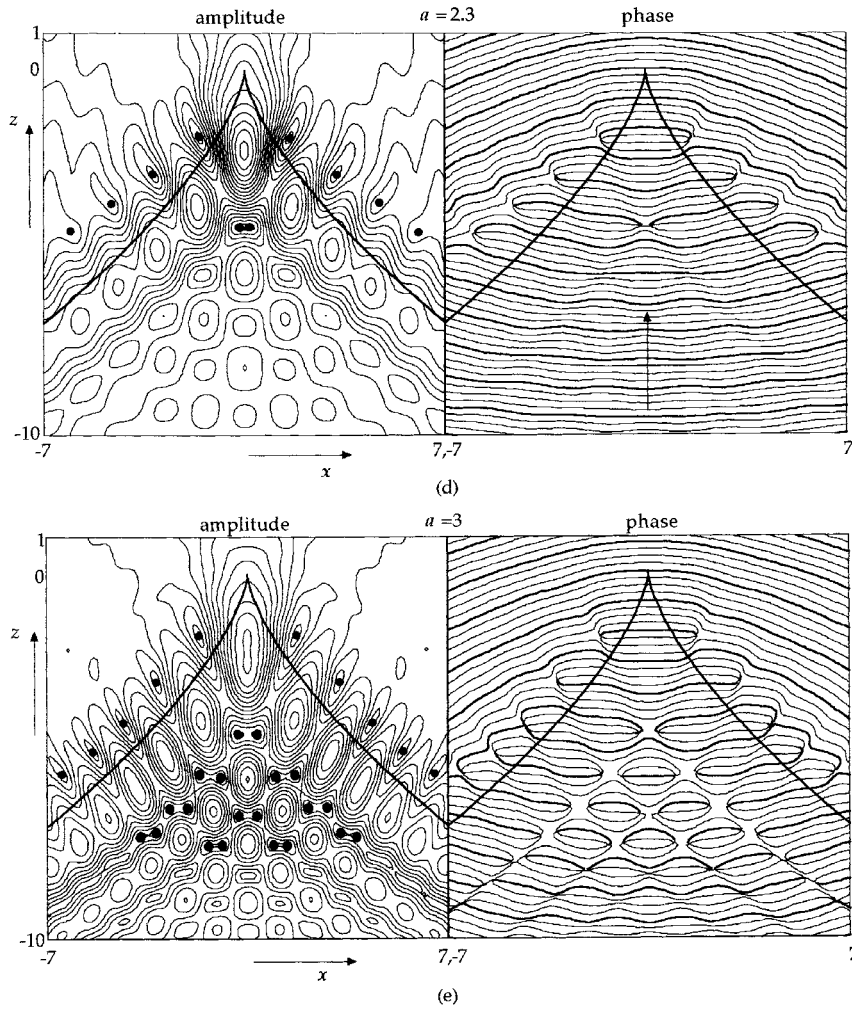


Figure 4. (Continued.)

The sign of  $\beta$  governs the sign of the aberration;  $\beta$  positive represents a cusp extending towards the lens and  $\beta$  negative a cusp extending away from the lens. We take  $\beta$  positive and deal with  $\beta$  negative later.

So far all the quantities have had physical dimensions. We now introduce dimensionless quantities,  $\xi, x, z$ , and make scalings designed to remove the factor  $k$  and the coefficient  $\beta$  in the exponent under the integral. Let  $\xi' = \xi_0 \xi, X = x_0 x, Z = z_0 z$ , and set  $\xi_0 = (4k\beta)^{-1/4}, x_0 = (k\xi_0)^{-1}, z_0 = (2k\xi_0^2)^{-1}$ . The exponent under the integral in (3) is then

$$-ik\phi = -ik(\beta\xi'^4 + Z\xi'^2 + X\xi') = -i(\frac{1}{4}\xi^4 + \frac{1}{2}z\xi^2 + x\xi).$$

$k$  and  $\beta$  have been removed and all quantities are now dimensionless. In terms of dimensionless  $K$ ,

$$K = \kappa z_0 = 2F^2 k z_0 = F^2 \xi_0^{-2} = 2F^2 (k\beta)^{1/2}, \quad (4)$$

the complex amplitude to be evaluated is

$$\psi(x, z) \propto e^{iKz} \int_{-a}^a \exp[-i(\frac{1}{4}\xi^4 + \frac{1}{2}z\xi^2 + x\xi)] d\xi, \quad (5)$$

where  $a = a'/\xi_0$  measures the half-aperture in dimensionless units. In the language of catastrophe theory,  $\xi$  is a state variable

while  $x, z$  are control variables. The only free parameters are  $a$  and  $K$ . If the limits were  $-\infty$  to  $+\infty$ , the integral would be the complex conjugate  $P^*(x, z)$  of the Pearcey integral  $P(x, z)$  as usually defined (Berry *et al* 1979, Berry 1992). Thus the problem reduces to evaluating the truncated Pearcey integral, which depends only on  $a$ , multiplied by a prefactor. The prefactor has no effect on the pattern of amplitude, but it does affect the phase pattern. At the same time, it is important to note that the positions of the dislocations (phase singularities) are identical, with and without the prefactor, because in both cases they are zeros of the amplitude. Since  $K \propto k^{1/2}$  by relations (4),  $K \rightarrow \infty$  with  $k$ , and there will be an increasingly large number of wavelengths between the focus and any given feature of the pattern at given  $x, z$ . Therefore, to display the phase pattern we must use a large but finite value of  $K$ . The evolution of the amplitude pattern is universal, under the control of  $a$ , but that of the phase pattern is not, because it depends also on  $K$ .

Because of this universality we present results in  $(x, z)$  space. The relation to physical space  $(x', z')$  is

$$x' = 2^{1/2} F k^{-3/4} \beta^{1/4} x, \quad z' = 2F^2 k^{-1/2} \beta^{1/2} z.$$

As  $k \rightarrow \infty$  the whole pattern streams anisotropically towards

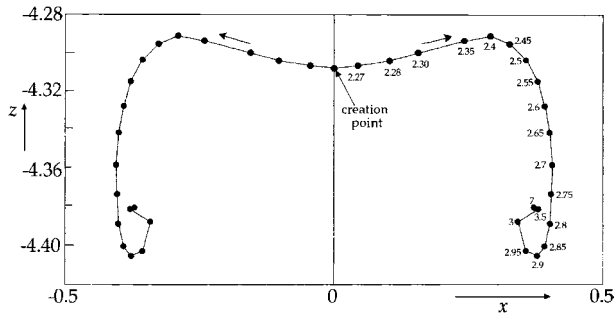


**Figure 5.** Trajectories of the first dislocation pair. After their birth on the axis they rapidly separate, following spiral paths to their final destinations in the full Pearcey pattern. The labels are the values of  $a$ .

the focus  $x' = z' = 0$ , as dictated by the different indices of  $k$  (the fringe indices) in the expressions for  $x'$  and  $z'$ .

There are two important limits to consider. The caustic of geometrical optics ( $k \rightarrow \infty$ ) is found from the ray condition  $\phi_x = 0$  together with the caustic condition  $\phi_{xx} = 0$  (Nye 1999) as

$$27x^2 = -4z^3.$$

When  $a$  is sufficiently small,  $\psi(x, z)$  becomes, apart from the phase prefactor,

$$\psi(x, z) \propto \int_{-a}^a e^{-ix\xi} d\xi = \frac{2 \sin(xa)}{x} \quad (6)$$

which is the standard Fraunhofer result for a narrow slit (figure 3).

The full Pearcey integral with infinite limits is difficult to compute (Berry 1992) because the integrand is highly oscillatory, but there is no corresponding problem when the integral is truncated at the modest values of  $a$  needed here. Figure 4 shows the amplitude and phase of  $\psi(x, z)$  for a fixed value  $K = 8$  and a range of  $a$ . With  $a$  small (figure 4(a)) one sees the central pair of an infinite row of wave dislocations with equal spacings  $\pi/a$  (the Fraunhofer pattern). Each is characterized by having zero amplitude and indeterminate phase; moreover, each has a phase saddle on its outer side, and on its inner side the beginning of an 'extra wavefront' which extends to join up with its partner on the other side to form an extra strip of wavefront. The rule for obtaining the position of the extra wavefront is first to identify the sense of circulation of the phase around the dislocation, for example, clockwise for all the dislocations to the right of the focus in figure 4(d); this sense is independent of the phase factor representing the carrier wave. On one side of the dislocation the phase gradient of the carrier wave will reinforce that close to the dislocation; this is the side for the extra wavefront. On the other side the phase gradients are opposed in sign; this is where the phase saddle will be found.

As  $a$  is increased, the cusp caustic begins to form and the Fraunhofer dislocations move inwards according to equation (6). The ends of the caustic come from the edges of the aperture. On further increase the caustic extends in length and the dislocations move downwards (figures 4(b) and (c)), eventually becoming the outer dislocations of the Pearcey

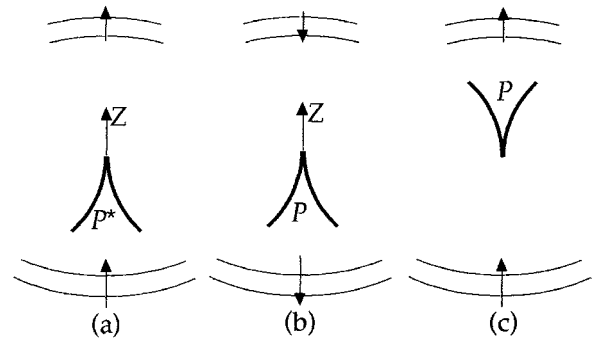


**Figure 6.** To show that the pattern for  $\beta$  negative is the same as for  $\beta$  positive except that it involves the Pearcey integral rather than its complex conjugate.

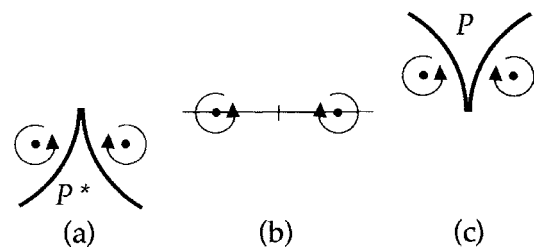


**Figure 7.** The sense of rotation for dislocations outside the caustic: (a)  $\beta$  positive, (b)  $\beta = 0$ , (c)  $\beta$  negative. The wave is travelling upwards throughout.

pattern (figures 4(d) and (e)). The caustic has a diffraction precursor: in figures 4(b) and (c) there are the first signs of what will ultimately be the row of maxima just inside the caustic even though the caustic itself is not yet present at these levels. The final Pearcey pattern contains additional close pairs of dislocations inside the caustic. As  $a$  increases these are created at places where the amplitude is small. The first pair (figure 4(d)) forms when  $a = 2.262381$  at  $x = 0$ ,  $z = -4.308110$ , to seven significant figures; they then rapidly separate, as traced in figure 5, following spiral paths to reach their eventual positions in the fully developed Pearcey pattern at  $x = \pm 0.374$ ,  $z = -4.378$ . While the first pair is separating, higher pairs are created successively, until eventually the whole Pearcey pattern is present. This outline of its evolution is the main result of the paper.

Since  $a = a'/\xi_0 = a'(4k\beta)^{1/4}$ , the patterns in figure 4 may be read either as a sequence with a fixed initial wavefront aberration given by  $\beta$  and an increasing aperture  $a'$ , or as an evolution with a fixed aperture and an increasing aberration. Notice how, as  $a$  increases, the principal maximum, which is centred on the focus for small  $a$ , moves to take up its position in the Pearcey pattern below the cusp point.

All this was for positive values of  $\beta$ . The corresponding result for negative values is readily seen through the diagrams in figure 6. Figure 6(a) shows diagrammatically the result for positive  $\beta$ , with the direction of increasing phase marked;  $P^*(x, z)$  is involved. Now take the conjugate complex of the whole  $\psi$ -pattern (figure 6(b)). This reverses all the phases and, more importantly, their gradients. Figure 6(c) is the same as 6(b) but inverted. It may be read as the same as the original scheme, but with the cusp pointing towards the lens rather

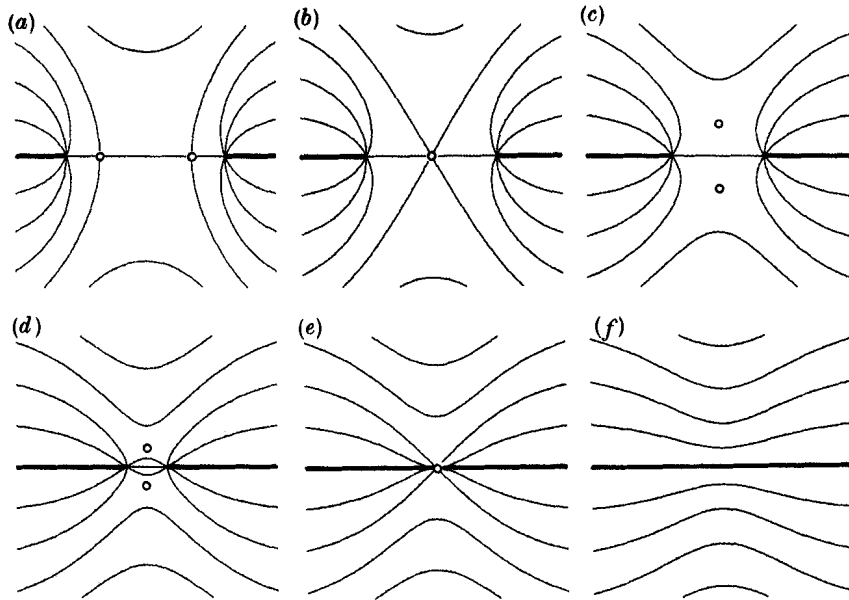


**Figure 8.** The symmetrical approach and annihilation of two dislocations of opposite sign with the saddles for phase initially, as in (a), on the line joining the dislocations. The equiphasal lines are at intervals of  $\frac{1}{4}\pi$  (from Nye *et al* 1988).

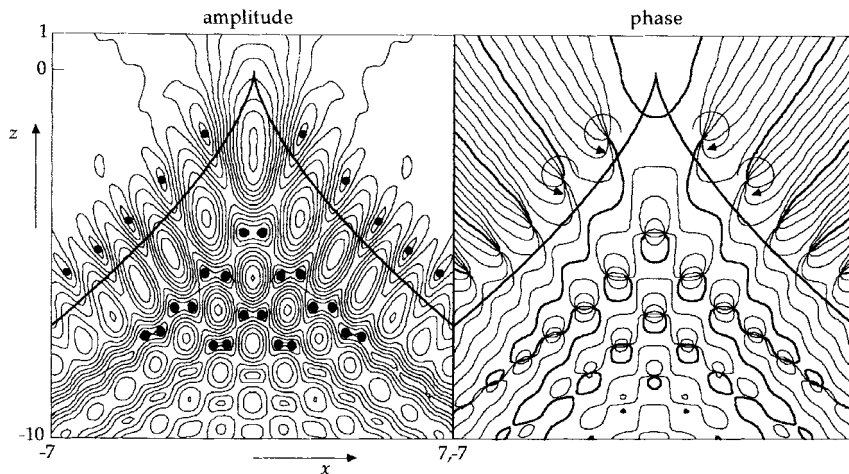


**Figure 9.**  $P^*(x, z)$ , without the prefactor, truncated at  $a = 3$ . Black dots mark zeros of amplitude.

than away from it, as would be given by negative  $\beta$ . Thus the pattern for negative  $\beta$  is the same as for positive  $\beta$ , except that it involves the Pearcey integral  $P(x, z)$  itself, rather than its complex conjugate.

As an example of the rule for the positions of the phase saddles and extra wavefronts, note that the first dislocation on the right outside the caustic in figure 4(e) has a clockwise circulation, also shown diagrammatically in figure 7(a). By the principle of structural stability, the same is true for the first dislocation on the right in the Fraunhofer pattern (figure 7(b)), with its extra strip of wavefront to its left. Proceeding further to negative  $\beta$ , this dislocation remains clockwise as shown in figure 7(c), and the extra wavefront is still to its left. But it now comes from  $P(x, z)$  rather than  $P^*(x, z)$ , so its circulation sense is reversed with respect to the caustic, as is seen in the diagram.

### 3. Pair creation and phase saddles

The role of phase saddles in the creation of a pair of wave dislocations deserves some attention. Two distinct topological indices have to be conserved in any reaction between dislocations. One is the Poincaré index  $n$ , which refers to the change in direction of the equiphasal lines on a circuit around the point in question; for dislocations or maxima  $n = +1$ , and for saddles  $n = -1$ . The other is the dislocation strength  $s$ , or topological charge; this takes the values  $\pm 1$ , according to the sense of circulation of the phase. It is shown in Nye *et al* (1988) that, in a two-dimensional wavefield obeying the wave equation

$$\frac{\partial^2 \psi}{\partial x'^2} + \frac{\partial^2 \psi}{\partial z'^2} + k^2 \psi = 0, \tag{7}$$

there can be no maxima or minima of phase. As a consequence,

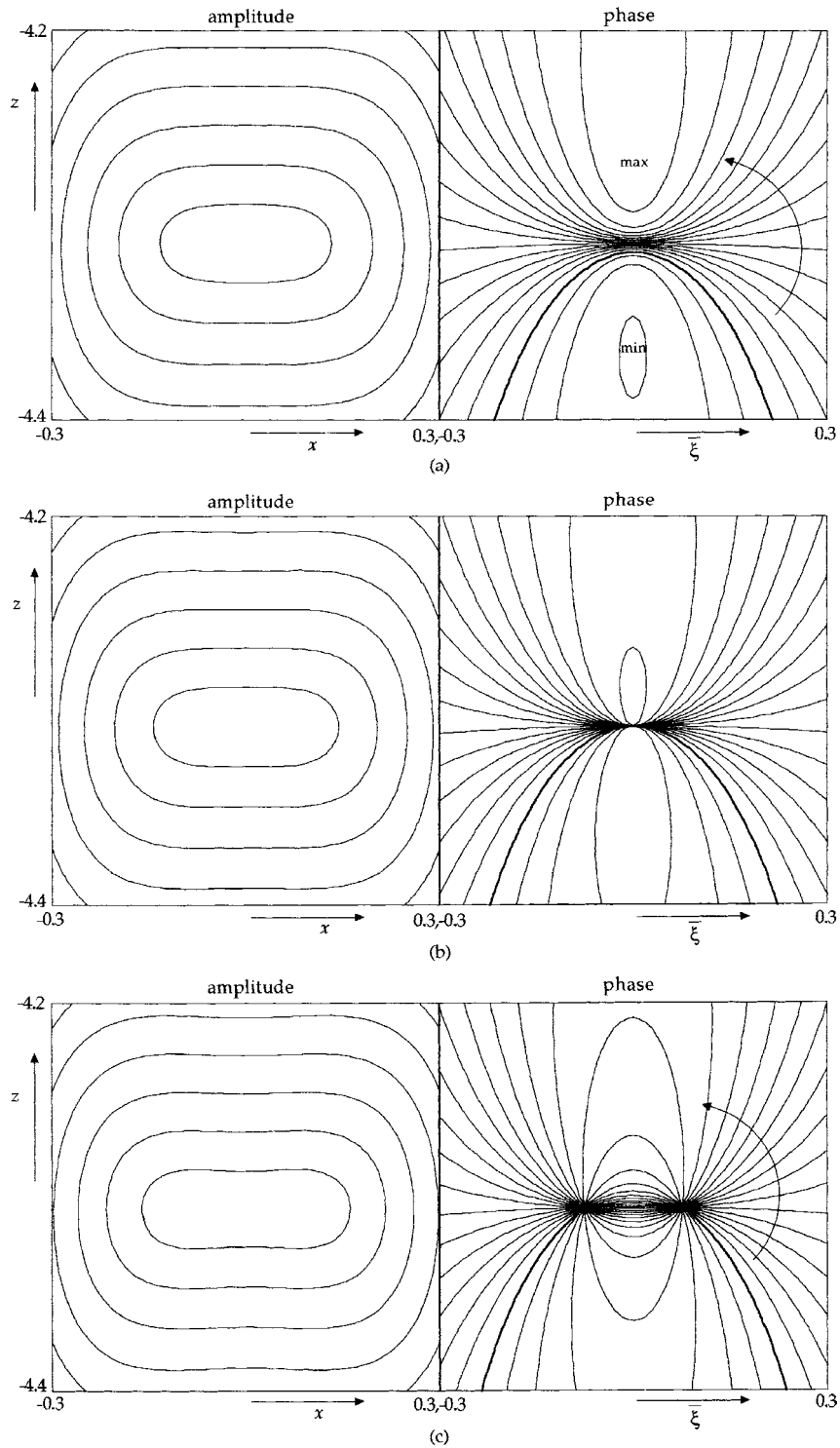


**Figure 10.** Close-ups of pair formation in the pattern of  $P^*(x, z)$  without the prefactor. (a)  $a = 2.2585$ , (b)  $a = 2.2624$ , (c)  $a = 2.27$ .

the only possible elementary reaction consistent with conservation of both  $n$  and  $s$  is the birth of two dislocations of opposite strength  $s = \pm 1$ , accompanied by the birth of two saddles—and the reverse event. It was further shown that, in the first stages of the creation event, the two associated saddles have to lie on a circle whose diameter is the line joining the two dislocations. This result ought to apply to the formation of the first pair of dislocations on the axis of the full Pearcey

pattern (i.e. including the prefactor) under the control of the parameter  $a$ . In fact the sequence is just that depicted in figure 4 of the above paper and reproduced here as figure 8. Increasing  $a$  corresponds to passing through the diagrams from (f) to (a) with the formation of a gap in the wavefronts. The two associated saddles (small circles) at first separate in the vertical direction and lie on the circle whose diameter joins the two dislocations; they reach a maximum separation and then return

to the horizontal axis, colliding to form a monkey saddle (b); finally they separate along the horizontal axis, and this is, in fact, their configuration in the limit of the full Pearcey pattern.

To verify that the saddles in the computed patterns do lie on the circle when close to the creation event, their positions were measured in the dimensionless variables  $(x, z)$  and transformed to the true space variables  $(x', z')$ . The scaling relations give for the ratio of intervals in  $x, z$

$$\frac{\Delta x}{\Delta z} = \frac{z_0}{x_0} \frac{\Delta X}{\Delta Z} = \frac{1}{2\xi_0} \frac{\Delta X}{\Delta Z} = \frac{F}{\xi_0} \frac{\Delta x'}{\Delta z'} = K^{1/2} \frac{\Delta x'}{\Delta z'}$$

and  $K$  for the computed pattern is known. We have seen that as  $k \rightarrow \infty$  there will be an increasingly large number of wavelengths between any given feature of the pattern, say the first pair, and the focus. On the other hand, for the circle result, the separation of the pair must be small compared with the wavelength. So the larger  $K$  is, the smaller must be the separation for the circle result, and so the closer  $a$  must be to the critical value for pair creation. The combinations  $K = 8$ ,  $a = 2.2642$ , and  $K = 16$ ,  $a = 2.2642$ , and  $K = 16$ ,  $a = 2.2700$  all give saddles in the predicted positions. The main source of error in the computed positions arises from the fact that normally no one of the computed phase lines passes exactly through a saddle.

The right-hand side of equation (5) consists of two parts, a phase prefactor followed by the complex conjugate of the truncated Pearcey integral. Figure 9 shows the wavefunction without the prefactor—choosing as an example  $a = 3$ , corresponding to figure 4(e). Because the prefactor only affects the phase, the positions of the phase singularities and the sense of their circulations are the same and so is the whole amplitude distribution. But the overall phase structure is quite different. In particular, notice that the phase structure of the uppermost dislocation pair on the axis is not at all the same as in figure 4(e). In fact, the pair are born quite differently, as is shown in figure 10. No saddles are involved; as  $a$  increases through the critical value, close inspection reveals a maximum above the creation point and a minimum below it (total Poincaré index +2) coming together very fast and being replaced by two dislocation points (each of index +1), so preserving the total index. The total strength  $s$  remains zero throughout.

The reason for this difference in phase behaviour between the complete wavefield and the truncated Pearcey integral is as follows. The wavefield (1), from which (5) is derived, obeys the wave equation (7), because it is a superposition of cylindrical wavelets, each obeying the wave equation when  $k\rho \gg 1$ . The theorem about the saddle behaviour and the approach to the circle depends on the fact that the wave equation does not allow maxima or minima. Although the truncated Pearcey integral happens to obey a certain paraxial wave equation, it does not obey the full wave equation (7). In consequence, maxima and minima are no longer prohibited and pair creation can take place without the participation of saddles.

## 4. Generalization

There is an important difference between the end-members of the sequence in figure 4. By the principles of catastrophe optics the cusp caustic is structurally stable. But the line focus of a perfect lens is not; indeed it can unfold in an infinite number of different ways, of which the cusp is just the simplest. For example, it could alternatively unfold into a butterfly catastrophe or a higher cuspid. The same applies to the perfect point focus, but here only a few of its more symmetrical unfoldings have been explored, mainly in terms of the singularity  $X_9$  (e.g. Nye 1999). All these unfoldings in geometrical optics are accompanied by changes to the corresponding diffraction patterns, which may be epitomized by their changing patterns of dislocations. There are therefore many different evolutionary paths to be explored for patterns of dislocations, starting from the row of dislocations for the line focus or from the circular Airy ring dislocations for the point focus, and ending with the various diffraction catastrophes. The elliptic umbilic diffraction catastrophe is studied from this point of view in Nye (2003). Actually, the starting point need not necessarily be the point focus; for example, for the elliptic umbilic catastrophe it could be the Fraunhofer pattern corresponding to a small triangular aperture, the parameter for the evolution being the size of the aperture. Other shapes of aperture would be appropriate for other catastrophes. Clearly there is much new territory here that could be explored and mapped.

## Acknowledgment

I am very grateful to Professor J H Hannay for much useful advice during the writing of this paper.

## References

- Berry M V 1992 Rays, wavefronts and phase: a picture book of cusps *Huygens' Principle 1690–1990: Theory and Applications* ed H Blok, H A Ferwerda and H K Kuiken (Amsterdam: North-Holland) pp 97–111
- Berry M V, Nye J F and Wright F J 1979 The elliptic umbilic diffraction catastrophe *Phil. Trans. R. Soc. A* **291** 453–84
- Connor J N L and Farrelly D 1981 Theory of cusped rainbows in elastic scattering: uniform semiclassical calculations using Pearcey's integral *J. Chem. Phys.* **75** 2831–46
- NIST Digital Library of Mathematical Functions 2004 (to be published on line)
- Nye J F 1999 *Natural Focusing and Fine Structure of Light* (Bristol: Institute of Physics Publishing)
- Nye J F 2003 From Airy rings to the elliptic umbilic diffraction catastrophe *J. Opt. A: Pure Appl. Opt.* **5** 503–10 (following article)
- Nye J F, Hajnal J V and Hannay J H 1988 Phase saddles and dislocations in two-dimensional waves such as the tides *Proc. R. Soc. A* **417** 7–20
- Pearcey T 1946 The structure of an electromagnetic field in the neighbourhood of a cusp of a caustic *Phil. Mag.* **37** 311–17